The Dynamics of Chromosome Movement in The Budding Yeast *Saccharomyces cerevisiae*

R. E. Palmer,*§ M. Koval,‡§ and D. Koshland§

*Department of Population Dynamics, Division of Reproductive Biology, Johns Hopkins University School of Hygiene and Public Health, Baltimore, MD 21205; ‡Department of Biology, Johns Hopkins University, Baltimore, Maryland 21218; and §Department of Embryology, The Carnegie Institution of Washington, Baltimore, Maryland 21210

Abstract. Nuclear DNA movement in the yeast, *Saccharomyces cerevisiae*, was analyzed in live cells using digital imaging microscopy and corroborated by the analysis of nuclear DNA position in fixed cells. During anaphase, the replicated nuclear genomes initially separated at a rate of 1 μm/min. As the genomes separated, the rate of movement became discontinuous. In addition, the axis defined by the segregating genomes rotated relative to the cell surface. The similarity between these results and those previously obtained in higher eukaryotes suggest that the mechanism of anaphase movement may be highly conserved. Before chromosome separation, novel nuclear DNA movements were observed in *cdc13*, *cdc16*, and *cdc23* cells but not in wild-type or *cdc20* cells. These novel nuclear DNA movements correlated with variability in spindle position and length in *cdc16* cells. Models for the mechanism of these movements and their induction by certain cdc mutants are discussed.

CHROMOSOME movement and spindle morphogenesis have been characterized in the budding yeast, *Saccharomyces cerevisiae*, by the cytological analysis of fixed cells (7, 24). In the mother cell, a short spindle forms between the spindle pole bodies (SPBs)[1] embedded in the nuclear envelope. After DNA replication, the nucleus migrates from its location in the mother cell to the isthmus, or "neck," between the mother cell and the bud. The spindle and nuclear envelope elongate through the neck into the bud, and one genome moves into the bud while the other remains in the mother cell. Once the genomes move to the distal regions of the mother cell and bud, the spindle breaks down, the nucleus divides, and cytokinesis is completed.

A virtue to studying chromosome movement in *S. cerevisiae* is the ability to isolate mutants that perturb mitosis. The molecular genetic analysis of these mutants may greatly expedite the identification and characterization of the cellular components necessary for chromosome movement. In this regard, temperature-sensitive mutations in *cdc13*, *cdc16*, *cdc20*, and *cdc23* genes are particularly interesting. At the nonpermissive temperature, these mutants arrest at a stage in the cell cycle after DNA replication: the nucleus has migrated to the neck between the mother cell and a large bud, and a short spindle has formed (24). The inability to discriminate individual mitotic chromosomes in yeast precludes directly assessing whether sister chromatids are still juxtaposed in these mutants (14). However, since the nuclear DNA appears as a single mass and the spindle fails to elongate extensively, these mutants are apparently defective in some step before or early in anaphase. Currently, it is unclear whether these mutants inhibit anaphase directly by affecting cellular components necessary for chromosome movement or indirectly by affecting other cellular processes that must be completed before yeast cells enter into anaphase.

A disadvantage to studying chromosome movement in yeast is the lack of a sensitive assay for studying chromosome movement in wild-type cells and potentially interesting mutants such as *cdc13*, *cdc16*, *cdc20*, and *cdc23*. Though the analysis of fixed cells has led to the identification of the major landmark events of mitosis, this approach has insufficient resolution for studying changes in chromosome position that occur within short intervals. Clearly, a more sensitive assay for chromosome movements involves following changes in chromosome position in live cells. In higher eukaryotes, chromosome movement can be followed in live cells with video microscopy because their chromosomes are visible with phase microscopy. Unfortunately, the inability to visualize yeast chromosomes with phase microscopy precludes this approach.

In this paper, we used digital imaging microscopy (DIM) (19) to follow the movement of fluorescently labeled nuclear DNA in live yeast cells. This new approach has allowed us to elucidate features of chromosome movement during anaphase of exponentially growing cells that were similar to those of higher eukaryotes. In addition, it revealed novel chromosome movement before anaphase in *cdc16* mutants. The distribution of nuclear DNA relative to the mother cell and bud in fixed *cdc16* cells not only confirmed the live cell

1. *Abbreviations used in this paper*: DAPI, 2,6,-diamidino-phenylindole; DIM, digital imaging microscopy; SPB, spindle pole body.

observations but provided us with a simple assay for determining that this novel chromosome movement also occurred in *cdc13*, *cdc20*, and *cdc23* mutants. The mechanism for generating the novel movement in *cdc16* cells was addressed by additional cytological studies.

Materials and Methods

Reagents

Rabbit anti-alpha and anti-beta tubulin were gifts from Dr. Frank Solomon (Massachusetts Institute of Technology, Cambridge, MA). FITC-conjugated goat antiserum to rabbit IgG was obtained from Cappel Laboratories (West Chester, PA). Calcofluor white M2R (Cellufluor) was obtained from Polysciences, Inc. (Warrington, PA), and 2,6,-diamidino-phenylindole (DAPI) was obtained from Boehringer Mannheim Biochemicals (Indianapolis, IN). Nocodazole (methyl-5-[2-thienylcarbonyl]-1-H-benzimidazole-2-yl-carbamate) was obtained from Aldrich Chemical Co. (Milwaukee, WI), and Zymolyase (100T) was purchased from ICN Immunobiologicals (Lisle, IL).

Strains

All *S. cerevisiae* strains were diploids and were isogenic with the strain A364A (15). The genotype of the wild-type strain was *MATa/MATα leu2/LEU2 his7/his7 hom3/HOM3 ADE2/ade2 ADE3/ade3 can1/can1 sap3/sap3 CYC2/cyc2*. Four homozygous, temperature-sensitive, cell division-cycle mutants were used: *cdc13*-1, *cdc16*-1, *cdc20*-1, and *cdc23*-1. Their genotypes were *MATa/MATα LEU2/leu2 his7/his7 hom3/HOM3 ADE2/ade2 ADE3/ade3 can1/can1 sap3/sap3*.

DIM

Chromosomal DNA can be observed when cells are stained with the DNA-specific fluorescent dye, DAPI. Cells exposed to room light grow at normal rates in the presence of DAPI; however, when cells are exposed to light from a 100-W mercury arc lamp, they stop dividing. By attenuating the amount of light from the mercury lamp to 1–3% of its normal intensity with neutral density filters and then amplifying the weakly emitted light by DIM (19), we were able to obtain time-lapse images of DNA movement in live cells. To prepare cells for microscopy, 25 ml of complete medium were inoculated with 1:1,000 vol of the appropriate saturated culture and grown overnight at 23°C to a density of 7×10^6/ml. DAPI was added to a final concentration of 2.5 μg/ml. 30 min after the addition of the stain, 18 μl of cells were placed on a flat slide and covered with a No. 1, 22-mm^2 coverslip. To analyze *cdc16*-1 cells recovering from arrest, cells were grown at 23°C to a density of 7×10^6/ml and then shifted to 36°C for 3 h. They were then allowed to recover for 10 min by returning them to 23°C, DAPI was added, and the stained cells were grown at 23°C for an additional 20 min. Cells were mounted on a slide as described above. Changes in nuclear DNA were observed using a 40× Neofluar objective (Carl Zeiss, Inc., Thornwood, NY) on a Universal microscope (Carl Zeiss, Inc.) equipped with epifluorescence optics suitable for DAPI-stained samples. A KS-1380 image intensifier (Videoscope International, Ltd., Washington DC) coupled to a Newvicon camera (Dage-MTI Inc., Michigan City, IN) was used to obtain video images of the cells. Exponentially growing cells with all the nuclear DNA in the mother and *cdc16*-1 cells recovering from arrest with the nuclear DNA all on one side of the neck were chosen for observation. Typically, both phase and fluorescence images were obtained at 2–5-min intervals. To minimize exposure, excitation light only illuminated the sample during image collection (~0.5–1 s/exposure). Four to eight video images were digitized and then boxcar-averaged using an IP-512 image processing system (Imaging Technology, Inc., Woburn, MA). Contrast was improved by removing background fluorescence from each fluorescence image followed by histogram equalization (13).

Cell Fixation and Culturing for Microscopy

Fresh cultures of cdc mutants were grown from saturated cultures that were diluted 1:1,000 in YPD medium (27). Cells were grown at the permissive temperature (23°C) to a density of 4×10^6/ml, and then an aliquot of these asynchronously growing cells was fixed immediately (23°C sample). To arrest cells, an aliquot was shifted to 36°C for 3 h, and the cells were examined with phase microscopy. For all mutants, >90% of the cells were arrested. An aliquot of these cells was fixed (23/36°C sample). The remaining cells were returned to the permissive temperature, allowed to recover for 30 min, and then fixed (23/36/23°C sample). Since wild-type cells continue to divide at 36°C, they were shifted to 36°C at a lower cell density (10^6/ml) to ensure that the cells were fixed at the same density as the cdc mutants. Cells were fixed for fluorescence, indirect immunofluorescence, and electron microscopy using a protocol that removed the cell walls (spheroplasting) before fixation. For each strain, 5 ml of cells were spun at 2,000 rpm for 2 min, resuspended in 1 ml of SCEM medium (1 M sorbitol, 10 mM sodium citrate, 60 mM EDTA, 0.1% 2-mercaptoethanol, pH 7), and spheroplasted for 5 min at 23°C with zymolyase (final concentration 30 μg/ml). Cells were fixed for 10 min by adding formaldehyde to a final concentration of 3.7% (wt/vol), spun at 5,000 rpm for 30 s, and rinsed with 1 ml of SK medium (1 M sorbitol and 50 mM KH_2PO_4). Cells were spun again, the supernatant was removed, and the pellet was resuspended in 70 μl of SK medium. Since cells that were arrested at 36°C were kept at 23°C for 7 min during spheroplasting, we also fixed cells at 36°C before spheroplasting. The nuclear morphology was similar for both treatments (data not shown).

Position of Nuclear DNA in the Mother Cell and Bud

Fixed cells were stained with calcofluor (50 μg/ml) to visualize the bud scar and DAPI (1 μg/ml) to visualize nuclear DNA. Both dyes were observed simultaneously with the same filter combination on an Axiophot microscope (Carl Zeiss, Inc.) with a 100× Neofluar objective (Carl Zeiss, Inc.). We defined three distinct nuclear staining patterns: the nuclear DNA was either (*a*) in the mother cell or the bud; (*b*) positioned approximately equally in the isthmus (neck) between the mother cell and the bud; or (*c*) had already segregated, with one genome in the mother cell and the other in the bud. Since both the bud scar and nuclear DNA were observed simultaneously, we focussed through the entire cell to ensure that we were scoring the structures properly. Between 50 and 300 cells per strain were scored, and representative cells were photographed with a 35-mm camera (Carl Zeiss, Inc.) with "hypered" Technical Pan film (Microfluor, Ltd., Stony Brook, NY).

Position of Microtubules and Nuclear DNA

Tubulin structures were visualized in *cdc16*-1 cells that were fixed while recovering from arrest using indirect immunofluorescence with an anti-tubulin antibody (21). Cells were also stained with DAPI and calcofluor as described above. In these experiments, cells were allowed to recover for only 15 min; however, the distribution of nuclear DNA was identical to that observed in the previous experiment. The position of the spindle in relation to the nuclear DNA and cell surface was scored in 100 cells. Although our fixing procedure also stained cytoplasmic microtubules, the spindle was discernable from cytoplasmic microtubules because it either appeared thicker or was positioned between the SPBs. The SPBs were observed as brightly stained spots that had microtubules radiating out toward the cell periphery. Spindle lengths were measured from enlargements of 35-mm negatives.

Electron Microscopy

Electron microscopy was performed on aliquots of the *cdc16*-1 cells that had been processed for indirect immunofluorescence microscopy (see above). After the formaldehyde fix, 50 μl of cells were mixed with an equal volume of 1.5% low melting-point agarose in SK medium, and the agarose was allowed to solidify at 4°C for 10 min. The agarose plugs were fixed in 2% glutaraldehyde in SK medium for 3 h at 23°C, rinsed twice in 0.1 M cacodylate buffer, pH 7.2, and placed in 1% OsO_4 plus 0.5% $K_3Fe(CN)_6$ in cacodylate buffer for 3 h at 23°C. Plugs were rinsed twice in 0.5 M maleate buffer and placed in 0.5% aqueous uranyl acetate in 0.5 M maleate buffer overnight at 4°C. After dehydration in a graded series of ethanol, the plugs were embedded in Epon plus nadic methyl anhydride/Quetol plus nonenyl succinic anhydride (6:4 ratio). Thin sections were stained with lead citrate and observed in an electron microscope (100s; JEOL USA, Peabody, MA).

Results

Nuclear DNA Movement in Exponentially Growing Cells

The movement of nuclear DNA in exponentially growing *S.*

cerevisiae cells was examined using DIM (see Materials and Methods). Cells were stained with the DNA-specific fluorescent dye, DAPI. Changes in the bud size and in the position of DAPI fluorescence were observed by recording phase and fluorescence images every 2–3 min. Two wild-type cells grown at 23°C, eight wild-type cells grown at 36°C and then shifted to 23°C, and seven *cdc16*-1 cells grown at the permissive temperature (23°C) were analyzed by this method. All these cells had similar chromosome segregation patterns.

From both the phase and fluorescence images of these cells, several general features of chromosome segregation were evident. The nuclear DNA appeared as a large mass (Fig. 1). During chromosome separation, the segregating nuclear genomes appeared slightly more punctate (Fig. 1, *I–K*), which may reflect clusters of partially condensed chromosomes. Additional small dots of fluorescence were observed around the bulk of the nuclear DNA. These dots are likely to be mitochondrial DNA, though a fraction of them may be small clusters of chromosomal DNA. During the 1–2 h of observation, the bud size increased (compare Fig. 1, *A* with *C*), indicating that bud growth continued under the coverslip. Furthermore, 16 of the 17 cells examined completed chromosome segregation. By these criteria, the physiology of the cells did not appear to be grossly affected by growth conditions under the coverslip or by the brief exposures to attenuated ultraviolet light necessary to produce fluorescence images. However, by the time nuclear segregation was completed, the bud size was often larger than what is normally observed in a population of fixed cells. Therefore, in these cells, the onset of anaphase may be delayed in relation to bud growth.

We determined the rate of chromosome segregation by measuring the distance between the centers of the segregating nuclear DNA masses as a function of time (Fig. 1, *E–O*). In two typical cells, the initial rate of separation was 0.6–1 μm/min, but, with time, the rate of separation appeared to decrease. In addition, the nuclear DNA appeared to pause several times, indicating that chromosomes may move in a discontinuous manner during anaphase (Fig. 2). However, we cannot exclude the possibility that when the DNA appeared to pause it was actually moving in a direction perpendicular to the focal plane.

We also assessed changes in the orientation of the axis of segregation (a line connecting the centers of the segregating genomes) relative to a reference axis bisecting the mother cell and bud (Fig. 1, *P–T*). In 70% of the cell divisions, the segregation axis was parallel to the reference axis as the nuclear DNA passed through the neck (Fig. 1 *P*) and then rotated to an oblique orientation (Fig. 1 *Q*). Occasionally, the segregation axis would oscillate between parallel and oblique orientations (Fig. 1, *R* and *S*) but, by the end of all mitoses, it was always parallel to the reference axis (Fig. 1 *T*). In the remaining cells, the segregation axis appeared to be parallel to the reference axis throughout anaphase. However, changes in the orientation of the segregation axis in these cells may have been obscured if the segregation axis rotated perpendicular to the plane of focus.

Nuclear DNA Movement in cdc16-1 Cells

When exponentially growing *cdc16*-1 cells are shifted from their permissive temperature (23°C) to the restrictive temperature (36°C) for 3 h, >90% of the cells arrest with large buds. When these cells are then shifted back to the permissive temperature, >95% of the cells recover and reenter the cell cycle. However, in recovering cells, the frequency of chromosome nondisjunction increases (Palmer, R. E., and D. Koshland, manuscript in preparation). This result prompted us to use DIM to examine nuclear DNA movements in 18 *cdc16*-1 cells that were recovering from arrest (see Materials and Methods).

While 15 of the 18 cells completed chromosome segregation, only 10 cells segregated their genomes in a pattern similar to exponentially growing cells. Seven cells exhibited novel nuclear DNA movements, where all, or nearly all, of the nuclear DNA passed from one side of the neck to the other (top cell in Fig. 3, *B–E*). In some cells, the nuclear DNA passed into the neck (bottom cell in Fig. 3 *C*) and then returned back to the side of the neck from which it started (bottom cell in Fig. 3 *G*). We refer to these movements as nuclear DNA transits. Nuclear DNA transits were not observed in either the eight wild-type cells exposed to the same temperature shift regime or the seven *cdc16*-1 cells grown at 23°C. This result suggests that the nuclear DNA transits were induced by the combination of the *cdc16* mutation and the temperature shift. Several nuclear DNA transits were observed in a given cell, indicating that the DNA could move across the neck either from the mother cell to the bud or vice versa. For a typical nuclear DNA transit, the DNA moved ~2 μm within 3–6 min. In the seven cells where nuclear DNA transits were observed, five cells subsequently entered into anaphase and completed chromosome segregation. The rate of chromosome separation in these cells (data not shown) was similar to that in exponentially growing wild-type or *cdc16*-1 cells (Fig. 2). Thus, nuclear DNA transits did not preclude subsequent completion of chromosome segregation or dramatically alter the rate of chromosome movement during anaphase.

Distribution of Nuclear DNA in Fixed Cells

To ensure that the observed nuclear DNA movements were not induced by DIM or by the growth conditions under the coverslip, we examined the distribution of nuclear DNA between the mother cell and bud in large numbers of fixed cells stained with both calcofluor and DAPI. Calcofluor stains chitin rings found at the neck of all dividing cells (16) and additional rings, bud scars, that are found exclusively on the surface of mother cells that have undergone previous divisions. Therefore, the distribution of the nuclear DNA between the mother cell and bud was determined unambiguously in fixed cells where a bud scar(s) was evident.

The distribution of nuclear DNA was similar for an exponentially growing population of wild-type cells, grown under three different temperature regimes, and an exponentially growing population of *cdc16*-1 cells, grown at 23°C (Table I). In budded cells, nuclear DNA was found predominantly on one side of the neck (58%) or segregated into both the mother cell and bud (38%) but rarely (4%) spanning the neck (Table I, part *A*). The doubling time for an exponentially growing population of cells is 150 min. We observed nuclear DNA passing through the neck in 2–3 min with DIM. Therefore, the fraction of cells with DNA spanning the neck should be ~1–2% (2/150), a value consistent with the

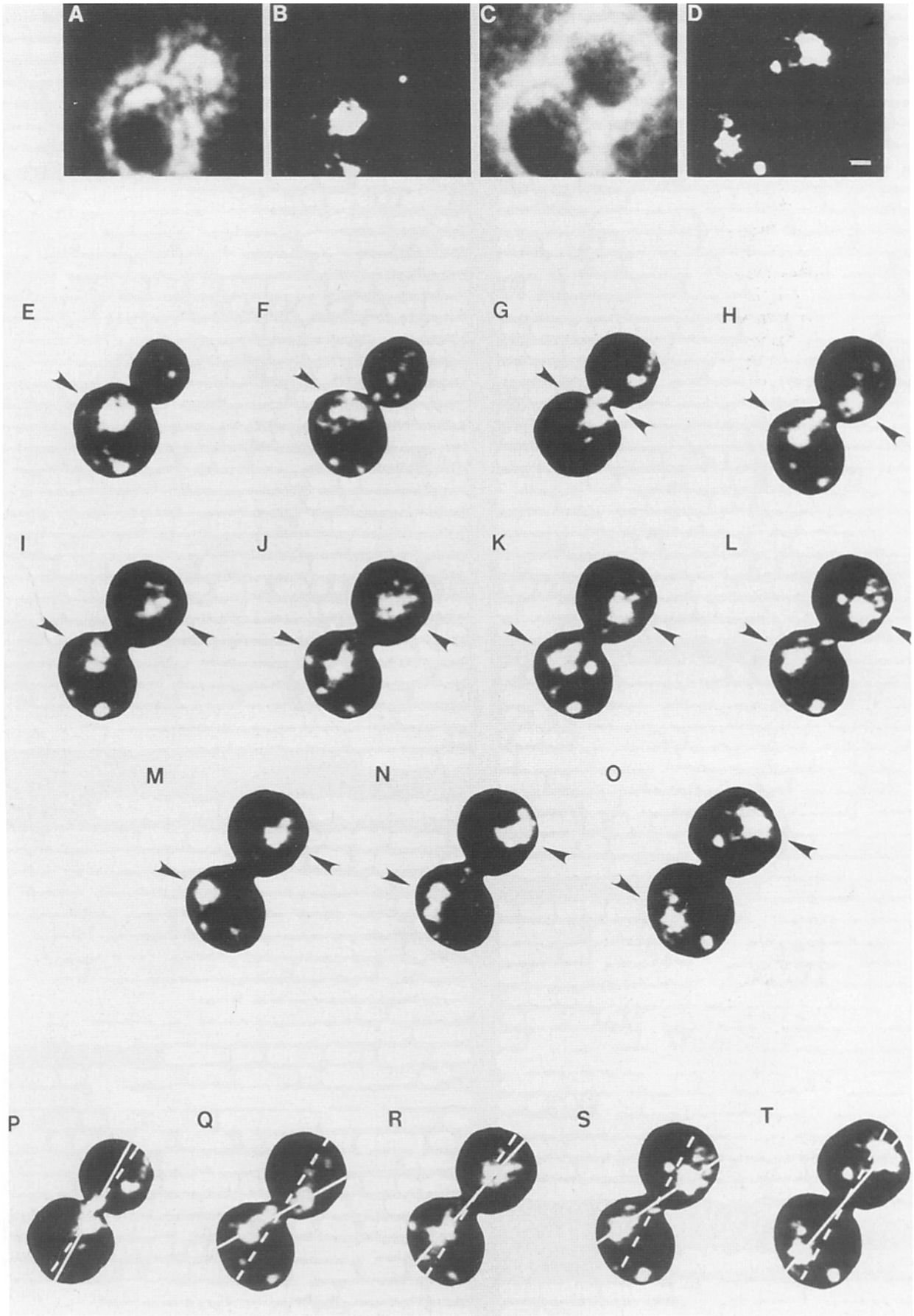
A
B
C
D
E
F
G
H
I
J
K
L
M
N
O
P
Q
R
S
T

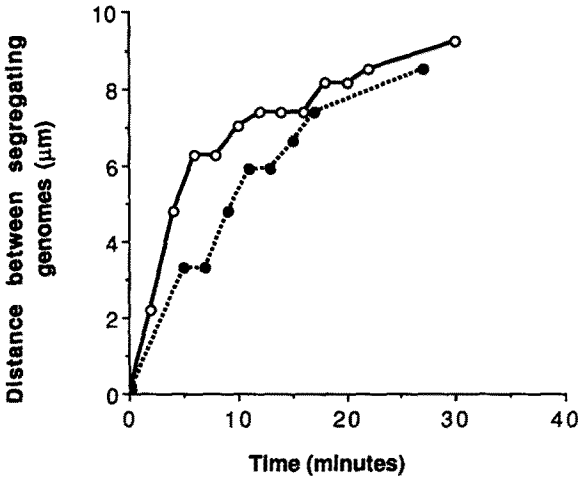

Figure 2. The segregation of nuclear DNA was followed in two exponentially growing cells using DIM (see Materials and Methods). The distance between the center of the two segregating genomes was measured from each fluorescence image. The separation of nuclear DNA was followed in one wild-type cell grown at 36°C then shifted to 23°C (*dotted line*) and one *cdcl6*-1 cell grown at 23°C, its permissive temperature (*solid line*).

fixed-cell result. In addition, only 1% of the budded cells with bud scars had the bulk of their DNA in the bud (Table I, part *B*). Therefore, nuclear DNA transits from the mother cell to bud are rare in exponentially growing cells as predicted from DIM.

We then examined the distribution of nuclear DNA in a population of budded *cdcl6*-1 cells recovering from arrest (see Materials and Methods). 65% of these cells had virtually all of the nuclear DNA on one side of the neck (Table I, part *A*, and Fig. 4, *b–d*). However, unlike the exponentially growing population of *cdcl6*-1 cells, half of the cells recovering from arrest had their nuclear DNA in the bud (Table I, part *B*, and Fig. 4, *c* and *d*), indicating that at least one nuclear DNA transit had occurred. Therefore, the fraction of total cells that had undergone at least one nuclear DNA transit before fixation was ~33%. This value was similar to that observed by DIM. Also, the fraction of cells with nuclear DNA spanning the neck was significantly higher in *cdcl6*-1 cells recovering from arrest compared with exponentially growing *cdcl6*-1 cells (data not shown) or wild-type cells (Table I, part *A*). This increase was predicted by DIM analysis where the DNA was frequently located in the neck as a result of nuclear DNA transits. Thus, the position of nuclear DNA in fixed *cdcl6*-1 cells recovering from arrest corroborates the nuclear DNA movements observed in these cells with DIM.

Nuclear Envelope and Spindle Structure in cdcl6 Cells Recovering from Arrest

Nuclear DNA transits in *cdcl6*-1 cells might occur by the movement of the nucleus across the neck or by the movement of chromosomes within the nucleus. We used electron microscopy to examine the morphology of the nuclear envelope in *cdcl6*-1 cells recovering from arrest. The morphology of the nuclear envelope was scored in longitudinal sections where both the mother cell and bud were of equal size to ensure that the plane of section was through the middle of the cell. The nucleus was unambiguously stretched across the neck in 26 of 27 cells examined (Fig. 5 *c*), suggesting that during a nuclear DNA transit chromosomes migrate across the neck within an extended nucleus.

The role of the spindle in generating nuclear DNA transits was examined in *cdcl6*-1 cells that were fixed while recovering from arrest. The position of the spindle in 100 cells was examined by indirect immunofluorescence using an anti-tubulin antibody. The spindle had three basic configurations: either it spanned the neck (Fig. 4 *e*), crossed the neck at an angle (Fig. 4 *f*), or was retained completely in the mother cell or bud (Fig. 4 *g*). The first two configurations were also observed in several electron micrographs (Fig. 5 *b*; data not shown). Therefore, in *cdcl6*-1 cells recovering from arrest, the position of the spindle was variable. In cells with all of the nuclear DNA in the mother cell, the spindle either crossed the neck directly or at an angle 90% of the time and was entirely within the mother cell the remaining 10%. Similarly, when the nuclear DNA was in the bud, the spindle spanned the neck 70% of the time and was entirely in the bud the remaining 30%. When the nuclear DNA spanned the neck, the spindle did also. The spindle and nuclear DNA were never observed in different parts of the cell. Thus, the colocalization of the spindle with the nuclear DNA is consistent with the idea that the spindle is responsible for directing DNA movement during nuclear DNA transits.

We measured the length of the spindle in cells recovering from *cdcl6* arrest (see Materials and Methods). The spindle exhibited variable lengths whether it spanned the neck or was confined entirely in the mother cell or bud (Fig. 6). Spindles spanning the neck were longer (4 ± 0.1 μm) than spindles contained entirely in the mother cell or bud (2.8 ± 0.07 μm). A small amount of this variability may result from the spindle being tilted relative to the plane of focus. However, the majority of spindles were measured from images where both SPBs were in focus. Given the narrow depth of field for the 100× objective, the maximum error in spindle length resulting from focusing artifacts would be 20%, which could not account for the 200% difference in spindle lengths observed. Thus, in cells recovering from *cdcl6*-1 arrest, the length and the position of the spindle were variable,

Figure 1. Time-lapse images of chromosome segregation in exponentially growing *S. cerevisiae* using DIM. Images are of *cdcl6*-1 cells growing at their permissive temperature, 23°C. *A* and *C* are phase images taken at the beginning (0 min) and end (70 min) of image collection, respectively. *B* and *D* are the fluorescence images of *A* and *C*, respectively. *E–O* are fluorescence images taken at the following time points: 0, 30, 32, 36, 40, 42, 44, 48, 52, 58, and 70 min, respectively. To view the movement of DNA relative to the periphery of the cell, a template of the periphery of the cell was made from each phase image (like those in *A* and *C*) and superimposed upon the corresponding fluorescence image. Arrows point to the nuclear DNA. *P–T* are the same images as *G*, *H*, *J*, *L*, and *O*, respectively; however, a reference axis (*dotted line*) and a segregation axis have been added. Bar, 1 μm.

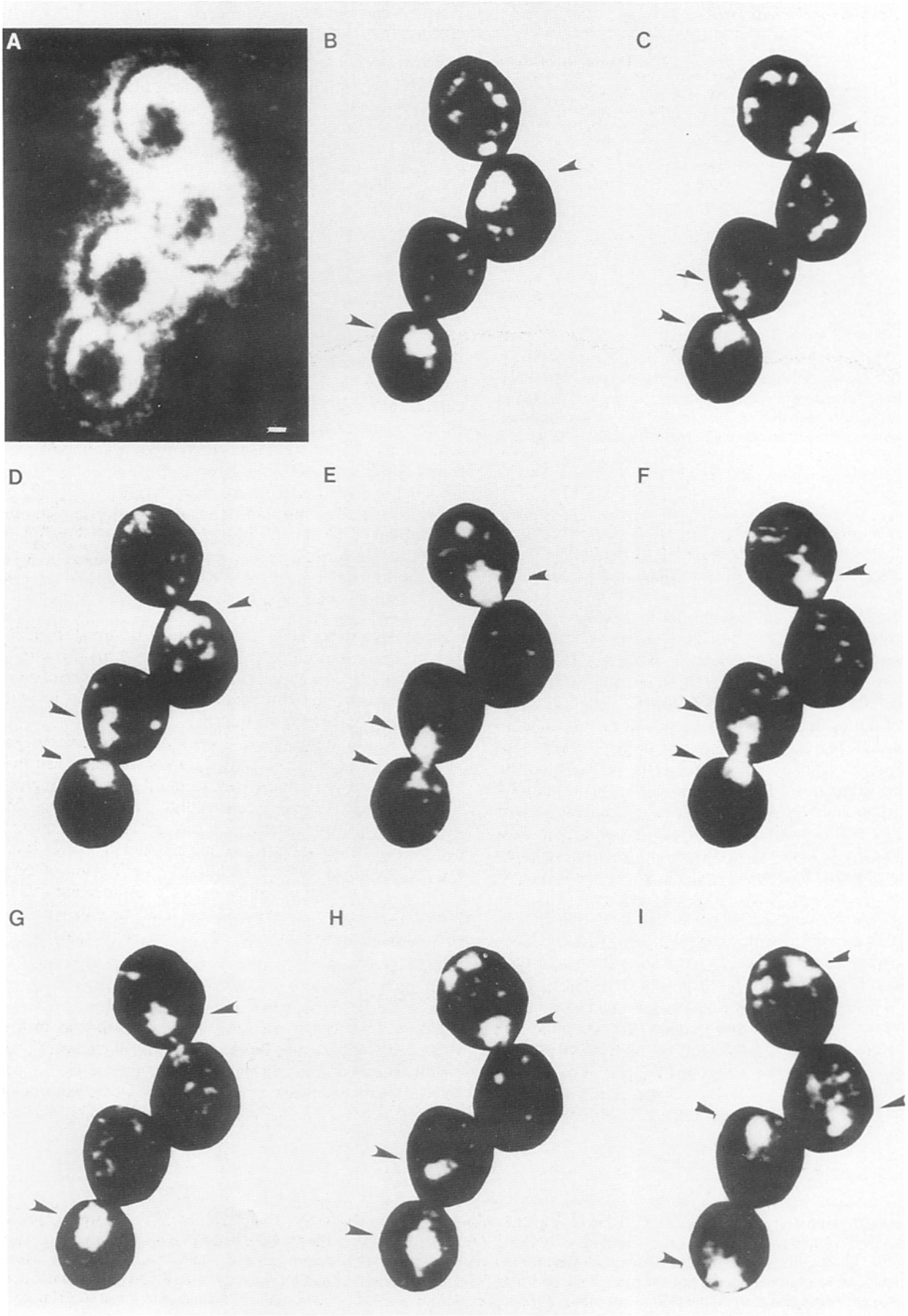
A
B
C
D
E
F
G
H
I

Table I. Position of Nuclear DNA

Strain	Temp	(A) position of nuclear DNA				(B) Position of nuclear DNA in budded cells with nuclear DNA on one side of the neck		
		On one side of neck	Through the neck	Segregated	Cells examined	Mother cell	Bud	Cells examined
	°C	%	%	%	*n*	%	%	*n*
Wild type	23	59.4	3.9	36.6	303	98.9	1.1	180
	23/36	55.6	3.6	40.6	300	98.8	1.2	167
	23/36/23	59.4	2.8	37.7	281	98.8	1.2	167
cdc16-1	23	–	–	–	–	99.1	0.9	104
	23/36	64.0	19.5	16.5	600	46.7	53.3	295
	23/36/23	63.3	22.2	14.5	600	49.9	51.1	90
cdc13-1	23	–	–	–	–	99.1	0.8	210
	23/36	73.4	26.3	0.3	300	24.1	75.9	369
	23/36/23	81.7	17.3	1.0	300	24.7	75.3	142
cdc23-1	23	–	–	–	–	99.0	1.0	100
	23/36	67.6	20.4	11.5	139	40.8	59.2	54
	23/36/23	70.2	21.7	8.1	161	37.0	63.0	46
cdc20-1	23	–	–	–	–	96.2	3.8	52
	23/36	88.8	3.1	8.1	320	96.6	3.4	265
	23/36/23	53.5	5.7	40.8	314	95.3	4.7	64

The position of the nuclear DNA was determined in fixed cells that were stained with DAPI to visualize DNA and calcofluor to visualize chitin. Cells with cdc mutations were fixed from an exponentially growing asynchronous population (23°C), from an arrested population (23/36°C), and from a population that was arrested and then allowed to recover from arrest for 30 min (23/36/23°C). Exponentially growing wild-type cells were subjected to the same temperature regimes. The nuclear DNA was located in three positions in the cell: on one side of the neck; through the neck between the mother cell and the bud; or segregated, with one genome located in the mother cell and the other in the bud (part *A*). In the cells where the nuclear DNA was on one side of the neck, we determined if the DNA was in the mother cell or the bud (see Materials and Methods) (part *B*).

which suggests that the spindle may exhibit dynamic movements within the elongated nucleus.

Nuclear DNA Transits in Other cdc Strains

To determine whether the induction of nuclear DNA transits was *cdc16* specific, the position of nuclear DNA in other cdc mutants was examined. We initially analyzed *cdc13*, *cdc20*, and *cdc23* mutants because they arrest with the same morphology as *cdc16* mutants (24). Cells were fixed while growing exponentially (23°C), while arrested (23/36°C), or while recovering from arrest (23/36/23°C), and the position of the nuclear DNA in the mother cell and bud was determined by staining with both calcofluor and DAPI (Materials and Methods).

The nuclear DNA morphology in *cdc13*-1 or *cdc23*-1 cells was similar to what had been observed in *cdc16*-1 cells (Table I, part *B*). Exponentially growing cultures, independent of the cdc mutation, had a small fraction of budded cells with the nuclear DNA entirely in the bud (1%). However, like *cdc16*-1 cells, >50% of *cdc13*-1 and *cdc23*-1 cells that were arrested or recovering from arrest had all the nuclear DNA in the bud (Table I, part *B*). These results suggest that nuclear DNA transits are enhanced when cells with these mutations are arrested or allowed to recover from arrest. In addition, ~20% of these cells had nuclear DNA through the neck (Table I, part *A*). As suggested above, the abundance of cells in this class may reflect the frequent passage of DNA into the neck during nuclear DNA transits.

On the other hand, *cdc20*-1 cells that were arrested or recovering from arrest had significantly different distributions of nuclear DNA than *cdc13*, *16*, or *23* cells. The fraction of *cdc20*-1 cells with all or nearly all of the nuclear DNA in the bud was only 4% in exponentially growing cells and did not increase in arrested cells or cells allowed to recover from arrest (Table I, part *B*). Furthermore, the fraction of cells with nuclear DNA through the neck did not increase (Table I, part *A*). These results suggest that arresting cells with this *cdc20* mutation does not induce nuclear DNA transits.

Discussion

We used DIM to examine chromosome movements in live yeast cells stained with the DNA-specific fluorescent dye, DAPI. This technique enabled us to determine the rate of chromosome separation and to observe subtle features of chromosome movement during anaphase, including changes

Figure 3. Time-lapse images of chromosome segregation in cells recovering from *cdc16* arrest using DIM. *cdc16*-1 cells were grown at 23°C, shifted to 36°C for 3 h to arrest cells, and then returned to 23°C to release cells from arrest. *A* is a phase image of the cells taken at the end of the observation period. Phase images taken at the beginning or at intermediate points (not shown) were indistinguishable. *B–I* are fluorescence images taken at the following time points: 0, 3, 12, 18, 36, 39, 40, and 70 min, respectively. To view the movement of DNA relative to the periphery of the cell, a template of the periphery of the cell was made from the phase image in *A* and superimposed upon the fluorescence images. Arrows point to the nuclear DNA. Bar, 1 μm.

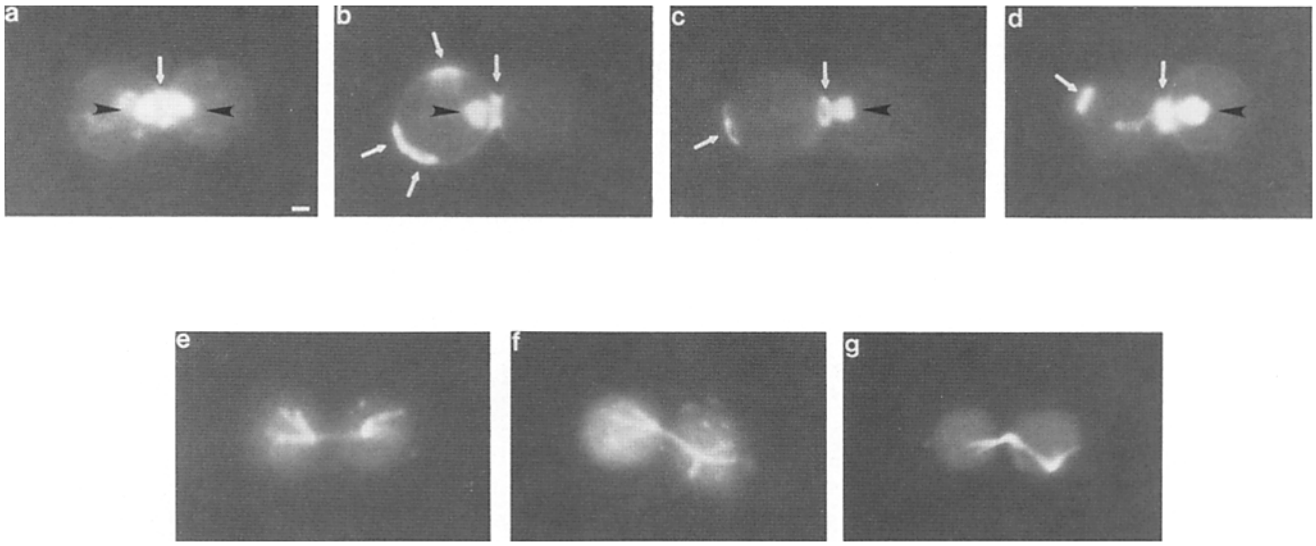

Figure 4. Fluorescence images of *cdcl6*-1 cells grown at 23°C, shifted to their restrictive temperature, 36°C, for 3 h, and then released from the arrest by returning them to 23°C for 15 min. Cells in *a–d* were fixed and stained with DAPI to visualize the nuclear DNA (*black arrowheads*) and calcofluor to visualize chitin (*white arrows*). Cells were observed with either the nuclear DNA passing through the isthmus, or neck, between the mother cell and bud (*a*); being retained in the mother cell, distinguished by chitin bud scars present on the cell surface (*b*); or being retained completely, or nearly completely, in the bud, determined by the absence of a bud scar (*c* and *d*). Cells in *e–g* are indirect immunofluorescence images of tubulin structures stained with anti-tubulin antibodies as described in Materials and Methods. The spindle is the structure observed between the SPBs, which are discernable in each cell as two brightly stained regions with cytoplasmic microtubules radiating out to the cell surface. The spindle was observed spanning the neck from mother cell to bud (*e*), spanning the neck at an angle (*f*), or located completely in the mother cell or bud (*g*). Bar, 1 μm.

in the orientation of the segregation axis and pauses in chromosome movement that were not previously identified in analyses of fixed cells. In addition, the analysis of cells recovering from *cdcl6* arrest revealed novel nuclear DNA movements (nuclear DNA transits) in which all, or nearly all, of the nuclear DNA moved from mother cell to bud or vice versa. Certain aspects of chromosome movement observed in wild-type and *cdcl6*-1 cells led to specific predictions about the distribution of nuclear DNA in fixed populations of these cells; these predictions were all substantiated, indicating that the DIM analysis reflects the normal, in vivo, state of the cells. The successful use of DIM to analyze wild-type and *cdcl6* cells suggests that this approach should be extremely helpful in analyzing other yeast gene products that may be required for chromosome movement during mitosis, karyogamy, or meiosis. Finally, if the punctate pattern of the nuclear DNA observed with DIM (Fig. 1) reflects small clusters of condensed mitotic chromosomes, then DIM may facilitate the analysis of chromosome morphogenesis in mitotic yeast.

Chromosome Movement in Exponentially Growing Cells

The kinetics of chromosome movement in exponentially growing yeast cells revealed several striking similarities to mitosis in higher eukaryotes. The rate of separation of the yeast genomes, 1 μm/min, is similar to that (1–3 μm/min) in PtK kangaroo rat cells (26) and in newt lung epithelial cells (NLC) (4). From our preliminary analysis, sister genomes did not separate from each other at a continuous rate; rather, several pauses appeared to occur. It is interesting to note that discontinuous movement of chromosomes has also been suggested in anaphase of NLC cells (4, 25).

During anaphase in yeast, the orientation of the segregation axis (a line between segregating genomes) changed relative to an axis through the neck. Several lines of evidence suggest that changes in the orientation of the segregation axis reflect changes in the orientation of the spindle. In exponentially growing cultures, the spindle of some cells is oriented in positions that are similar to the locations of the segregation axis (Palmer, R. E., and D. Koshland, unpublished results). In addition, the rotation of the spindle has been observed during prometaphase in NLC cells (4), during metaphase in other fungi (1, 2), and during telophase in guard mother cells of *Allium cepa* (22). Interestingly, these changes in the orientation of the yeast spindle during anaphase may not be random. In the 70% of cells where the orientation of the segregation axis changed, the axis (and presumably the spindle) always rotated during or just after the DNA crossed the neck. This specific reorientation of the segregation axis may not have been observed in 30% of the cells because in these cells rotation occurred in a plane perpendicular to the plane of focus. Programmed reorientation of spindles is a common feature of mitosis in other fungi (1), stomatal differentiation in *Allium cepa* (22), and embryogenesis in *Caenorhabditis elegans* (18).

Morphological differences between yeast and higher eukaryotic cells during mitosis suggest that some aspects of mitosis differ between these cell types. For example, during mitosis in yeast, the nuclear envelope does not breakdown, and the spindle has very few kinetochore or pole-to-pole microtubules (23). However, recent experiments suggest that a high degree of structural and functional similarity exists between the maturation-promoting factor of *Xenopus laevis*, the *cdc2*$^+$ gene product of *Schizosaccharomyces pombe*, and the *CDC28* gene product of *Saccharomyces cerevisiae*. This fact suggests that molecules that regulate the cell cycle

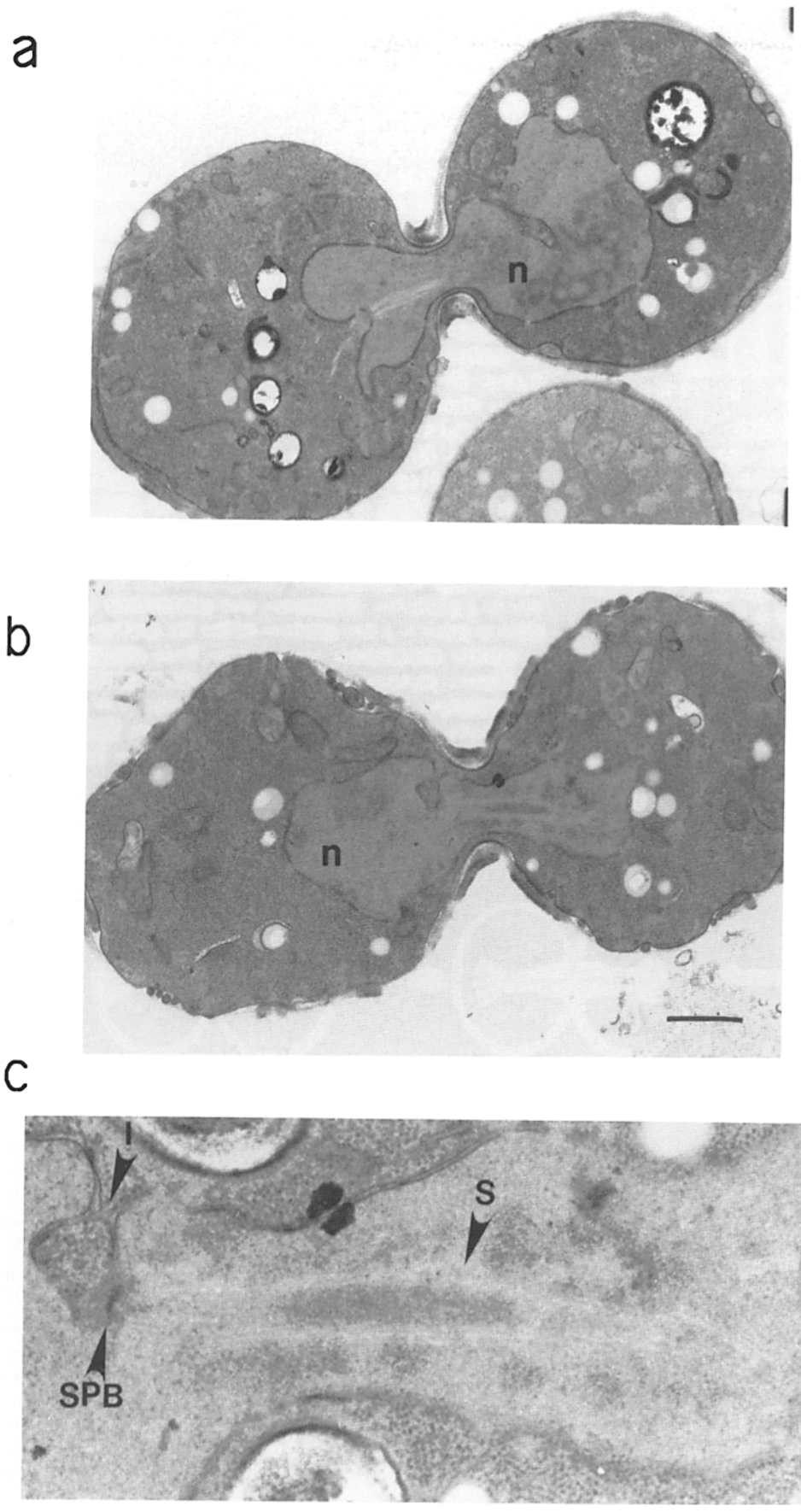

Figure 5. Electron micrographs of *cdc16*-1 cells that were shifted to their restrictive temperature, 36°C, for 3 h to arrest them and then released from their arrest by returning the cells to 23°C for 15 min. *a* and *b* are different cells where the nucleus (*n*) is stretched across the neck between the mother cell and bud. *c* is an enlargement of *b*. Note invagination (*l*) of the nuclear envelope where the SPB is attached to the nuclear envelope. The spindle (*S*) almost completely crosses the nucleus. Bar: (*a* and *b*) 1 μm; (*c*) 3.5 μm.

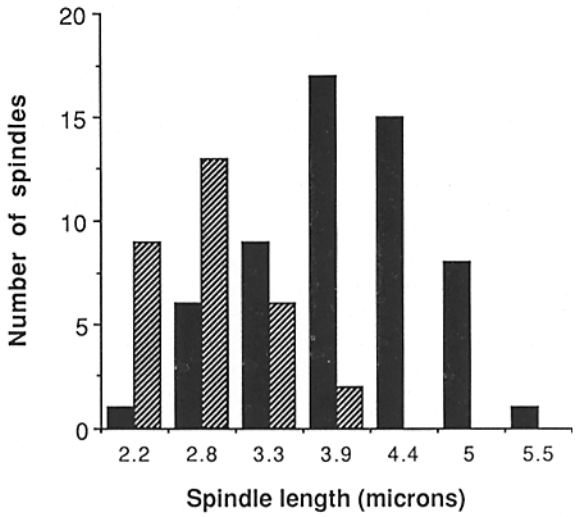

Figure 6. Spindle lengths of *cdcl6*-1 cells that were shifted to their restrictive temperature, 36°C, for 3 h and then released from the arrest by returning the cells to 23°C for 15 min. Lengths were measured from enlargements of 35-mm negatives only from cells in which both SPBs were discernable. The spindle lengths were classified into two groups: those spindles that crossed the neck from the mother cell to bud (*solid bars*) and those cells where the spindle was retained completely in the mother cell or bud (*stippled bars*).

are highly conserved (3, 5, 6, 10–12). Furthermore, from the data presented in this study, the three most striking observations of yeast anaphase are the absolute rate of chromosome separation, the pauses in chromosome separation, and the apparent rocking of the spindle. All of these features have precedents in anaphase of higher eukaryotes, suggesting that the mechanism of chromosome movement during anaphase may be conserved between yeast and higher eukaryotes.

Nuclear DNA Transits

We observed nuclear DNA transits in cells recovering from *cdcl6*-1 arrest. Any hypothesis on the mechanism of these transits must take into account the morphological features of cells undergoing these transits, including the presence of an elongated nucleus extending into both the mother cell and bud, variability in the length and position of the spindle, and colocalization of the nuclear DNA with the spindle. Since the nucleus is elongated between the mother cell and bud, nuclear DNA transits are occurring by a mechanism that moves chromosomes within the nucleus. It is reasonable to suggest that the spindle directs chromosome movement during nuclear DNA transits given the observed colocalization of the spindle and chromosomes and the apparent role of the spindle in moving chromosomes within the nucleus during anaphase (17). We propose two models to explain how the position of the spindle and the associated chromosomes may change (Fig. 7). In model I, the spindles may undergo a series of asymmetric expansions and contractions that cause them to move to a new position within the nucleus. Changes in spindle microtubule lengths have been associated with oscillatory movement of individual chromosomes during prometaphase/metaphase in higher eukaryotes (4, 25). Alternatively (model II), the spindles may have fixed lengths and their positions in the nucleus may change by extranu-

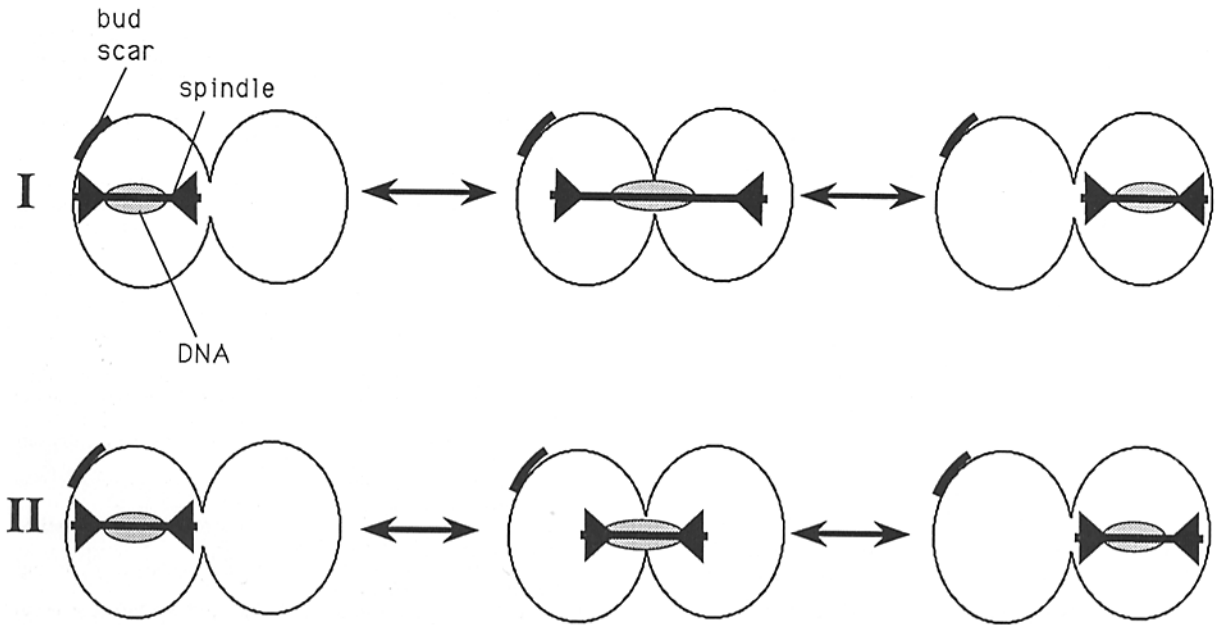

Figure 7. Mechanism of nuclear DNA transits. Two models to explain the role of the spindle in nuclear DNA transits are presented. In model I, the right SPB (*solid triangle*) expands through the neck. As the spindle expands, the nuclear DNA moves into the neck. When the left spindle pole collapses toward the neck, the nuclear DNA moves into the bud. Alternatively, when the right pole collapses toward the neck, the nuclear DNA moves back into the mother cell. In model II, the spindle is fixed in length. Nuclear DNA transits occur by migration of the whole spindle to the neck. When the spindle continues to migrate into the bud, nuclear DNA moves into the bud. Alternatively, when the spindle migrates back into the mother, nuclear DNA migrates back into the mother. In this figure, the cytoplasmic microtubules and the nuclear envelope are omitted for clarity. It should be noted that the extensive elongation of the nuclear envelope into the mother and bud (Fig. 5) does not appear to constrain the position of the SPBs in the cell. In particular, the SPBs can occupy a position proximal to the neck by sitting on invaginations of the nuclear envelope (see Fig. 5).

clear forces, perhaps exerted through cytoplasmic microtubules that emanate from the SPBs. This model has been proposed for prometaphase/metaphase nuclear DNA movements in other fungi (2). We prefer model I because it explains the observed variability in spindle lengths; however, we cannot exclude the possibility that *cdcl6* cells arrest with variable spindle lengths that remain fixed until the onset of anaphase.

The position of nuclear DNA in fixed cells indicated that nuclear DNA transits are rarely seen in wild-type cells but are enhanced in *cdcl3*, *cdc23*, and *cdcl6* strains that were arrested or allowed to recover from arrest. It is possible that these mutants all induce transits because they affect proteins directly required for proper chromosome movement. In fact, the products of *CDCl6* and *CDC23* share amino acid homology and may be functionally related (Sikorski, R., and P. Heiter, personal communication). However, genetic analysis of the *CDCl3* gene suggests that its product may be required for DNA metabolism (Weinert, T., and L. Hartwell, personal communication). Furthermore, nuclear DNA transits occur in *cdcl7* cells (Palmer, R. E., and D. Koshland, unpublished results) that have a defect in DNA polymerase (9). Therefore, it seems unlikely that all these mutants induce nuclear DNA transits because they are defective in some component of the segregation apparatus.

As an alternative model, nuclear DNA transits in some of these mutants may result from the oscillation of chromosomes that occur normally during prometaphase and metaphase. In fact, in other eukaryotes, chromosome oscillation has been observed during these stages of mitosis (1, 2, 4, 25). We suggest two explanations why these oscillations frequently give rise to nuclear DNA transits in cells arrested before anaphase but infrequently in exponentially growing cells. One possibility is that prometaphase and metaphase are sufficiently short in exponentially growing cells that these cells usually enter anaphase before an oscillation results in a nuclear DNA transit. On the other hand, cells arrested before anaphase have ample time to complete transits. Alternatively, the magnitude of chromosome oscillation in exponentially growing cells may be insufficient to cause a transit. However, prolonged arrest of cells before anaphase may cause the magnitude to become sufficiently exaggerated to generate nuclear DNA transits.

Cells arrested by a *cdc20* mutation fail to undergo nuclear DNA transits. In addition, cells arrested with the microtubule-depolymerizing drug, nocodazole, also fail to undergo nuclear DNA transits (our unpublished results and reference 20). The failure to observe nuclear DNA transits in nocodazole-treated cells is not surprising since the nucleus cannot migrate to the neck and, thus, remains entirely in the mother cell (20). The failure to observe nuclear DNA transits in a *cdc20* mutant is more interesting since this mutant, like *cdcl6*, *cdcl3*, and *cdc23*, arrests before the onset of anaphase with the nucleus spanning the neck and a short spindle (8). In addition, our preliminary results suggest that cells released from *cdc20* arrest appear to commence chromosome separation immediately, suggesting a direct involvement between the *CDC20* gene product and the movement of chromosomes during anaphase. One possibility is that the *cdc20* cells may arrest at a stage in the cell cycle after nuclear DNA transits can take place but before the onset of anaphase. Alternatively, the *CDC20* gene product may be directly required for chromosome movement: e.g., a component of the spindle that directs proper assembly of microtubules, a component of the kinetochore necessary for microtubule binding, or a component of a mitotic motor. To address if the gene product has any of these functions, we are analyzing other mutant alleles of the *CDC20* gene as well as cloning the wild-type gene.

We thank Michael Sepanski for technical assistance and Dick Pagano for the use of the image processor. We are grateful for the critical evaluation of the manuscript by Joseph G. Gall and Forrest Spencer. Christine Norman and Shirley Whitaker assisted with the preparation of the manuscript, and Connie Jewell helped with the figures.

R. E. Palmer was supported by National Institutes of Health training grant HD07276 awarded to the Department of Population Dynamics, Division of Reproductive Biology, and a Howard Hughes predoctoral grant awarded to the Carnegie Institution of Washington. M. Koval was supported by National Institutes of Health grant GM37434. D. Koshland is a Lucille P. Markey Scholar, and this work was supported in part by a grant from the Lucille P. Markey Charitable Trust.

Received for publication 28 July 1989 and in revised form 8 September 1989.

References

1. Aist, J. R. 1969. The mitotic apparatus in fungi, *Ceratocysitis fagacearum* and *Fusarium oxysporum*. *J. Cell Biol.* 40:120–135.
2. Aist, J. R., and M. W. Berns. 1981. Mechanics of chromosome separation during mitosis in *Fusarium* (fungi imperfecti): new evidence from ultrastructural and laser microbeam experiments. *J. Cell Biol.* 91:446–458.
3. Arion, D., L. Meijer, L. Brizuela, and D. Beach. 1988. cdc 2^+ is a component of the M phase–specific histone H1 kinase: evidence for identity with MPF. *Cell.* 55:371–378.
4. Bajer, A. S. 1982. Functional autonomy of monopolar spindle and evidence of oscillatory movement in mitosis. *J. Cell Biol.* 93:33–48.
5. Beach, D. H., B. Durkacz, and P. M. Nurse. 1982. Functionally homologous cell cycle control genes in budding and fission yeast. *Nature (Lond.).* 300:706–709.
6. Booher, R., and D. Beach. 1986. Site-specific mutagenesis of $cdc2^+$, a cell cycle control gene of the fission yeast *Schizosaccharomyces pombe*. *Mol. Cell. Biol.* 6:3523–3530.
7. Byers, B. 1981. Cytology of the Yeast Life Cycle. *In* Molecular Biology of the Yeast Saccharomyces: Life Cycle and Inheritance. J. N. Strathern, E. W. Jones, and J. R. Broach, editors. Cold Spring Harbor Laboratory, Cold Spring Harbor, NY. 59–96.
8. Byers, B., and L. Goetsch. 1974. Duplication of spindle plaques and integration of the yeast cell cycle. *Cold Spring Harbor Symp. Quan. Biol.* 38:123–131.
9. Carson, M. J. 1987. CDC17, the structural gene for DNA polymerase I of yeast: mitotic hyperecombination and effects on telomere metabolism. Ph.D. thesis. University of Washington, Seattle, WA. 110 pp.
10. Draetta, G., F. Luca, J. Westendorf, L. Brizuela, J. Ruderman, and D. Beach. 1989. cdc2 protein kinase is complexed with both cyclin A and B: evidence for proteolytic inactivation of MPF. *Cell.* 56:829–838.
11. Dunphy, W. G., L. Brizuela, D. Beach, and J. Newport. 1988. The *Xenopus* homolog of $cdc2^+$ is a component of MPF, a cytoplasmic regulator of mitosis. *Cell.* 54:423–431.
12. Gautier, J., C. Norbury, M. Lohka, P. Nurse, and J. Maller. 1988. Purified maturation-promoting factor contains the product of *Xenopus* homolog of the fission yeast cell cycle control gene $cdc2^+$. *Cell.* 54:433–439.
13. Gonzales, R. C., and P. Wintz. 1987. Digital Image Processing. Addison-Wesley Publishing Co., Reading, MA. 503 pp.
14. Gordon, C. N. 1977. Chromatin behaviour during the mitotic cell cycle of *Saccharomyces cerevisiae*. *J. Cell Sci.* 24:81–93.
15. Hartwell, L. H. 1967. Macromolecule synthesis in temperature-sensitive mutants of yeast. *J. Bacteriol.* 93:1662–1670.
16. Hayashibe, M., and S. Katohda. 1973. Initiation of budding and chitin ring. *J. Gen. Appl. Microbiol.* 19:23–31.
17. Huffaker, T. C., J. H. Thomas, and D. Botstein. 1988. Diverse effects of beta-tubulin mutations on microtubule formation and function. *J. Cell Biol.* 106:1997–2010.
18. Hyman, A. A., and J. G. White. 1987. Determination of cell division axes in the early embryogenesis of *C. elegans*. *J. Cell Biol.* 105:2123–2135.
19. Inoue, S. 1986. Video Microscopy. Plenum Publishing Corp., New York. 584 pp.
20. Jacobs, C. W., A. E. M. Adams, P. J. Szaniszlo, and J. R. Pringle. 1988. Functions of microtubules in the *Saccharomyces cerevisiae* cell cycle. *J. Cell Biol.* 107:1409–1426.
21. Kilmartin, J. V., and A. E. M. Adams. 1984. Structural rearrangements of tubulin and actin during the cell cycle of the yeast *Saccharomyces*. *J.*

Cell Biol. 98:922–933.
22. Palevitz, B. A. 1974. The control of the plane of division during stomatal differentiation in allium. II. Drug studies. *Chromosoma (Berl.).* 46:297–326.
23. Peterson, J. B., and H. Ris. 1976. Electron microscopic study of the spindle and chromosome movement in the yeast *Saccharomyces cerevisiae*. *J. Cell Sci.* 22:219–242.
24. Pringle, J. R., and L. H. Hartwell. 1981. The *Saccharomyces cerevisiae* Cell Cycle. *In* The Molecular Biology of the Yeast *Saccharomyces*: Life Cycle and Inheritance. J. N. Strathern, E. W. Jones, and J. R. Broach, editors. Cold Spring Harbor Laboratory, Cold Spring Harbor, NY. 97–142.
25. Rieder, C. L., E. A. Davison, C. W. Jensen, L. Cassimeris, and E. D. Salmon. 1986. Oscillatory movements of chromosomes and their position relative to the spindle pole result from the ejection properties of the aster and half-spindle. *J. Cell Biol.* 103:581–591.
26. Roos, U. P. 1973. Light and electron microscopy of rat kangaroo cells in mitosis. II. Kinetochore structure and function. *Chromosoma (Berl.).* 41:195–220.
27. Sherman, F., G. R. Fink, and J. B. Hicks. 1986. Methods in Yeast Genetics. Cold Spring Harbor Laboratory, Cold Spring Harbor, NY. 186 pp.